NANO LETTERS

pubs.acs.org/NanoLett Letter

# Intense Dark Exciton Emission from Strongly Quantum-Confined $CsPbBr_3$ Nanocrystals

Daniel Rossi, Xiaohan Liu, Yangjin Lee, Mohit Khurana, Joseph Puthenpurayil, Kwanpyo Kim, Alexey V. Akimov, Jinwoo Cheon,* and Dong Hee Son*

Cite This: *Nano Lett.* 2020, 20, 7321−7326 Read Online

ACCESS | Metrics & More | Article Recommendations | Supporting Information

**ABSTRACT:** Dark exciton as the lowest-energy (ground) exciton state in metal halide perovskite nanocrystals is a subject of much interest. This is because the superior performance of perovskites as the photon source combined with long lifetime of dark exciton can be attractive for many applications of exciton. However, the direct observation of the intense and long-lived dark exciton emission, indicating facile access to dark ground exciton state, has remained elusive. Here, we report the intense photoluminescence from dark exciton with microsecond lifetime in strongly confined $CsPbBr_3$ nanocrystals and reveal the crucial role of confinement in accessing the dark ground exciton state. This study establishes the potential of strongly quantum-confined perovskite nanostructures as the excellent platform to harvest the benefits of extremely long-lived dark exciton.

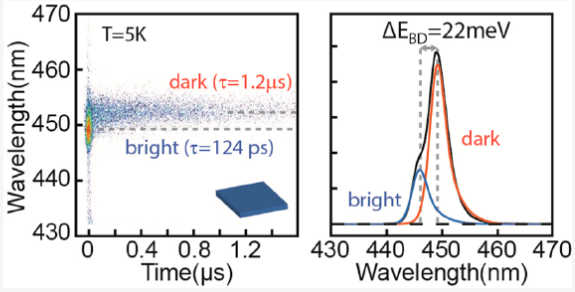


**KEYWORDS:** *$CsPbBr_3$ Perovskite, Strong Confinement, Dark Exciton*

## INTRODUCTION

Metal halide perovskite (MHP) nanocrystals (NCs) have gained explosive interest as a superior source of photons and charges with high luminescence quantum yield and long carrier diffusion length compared to many other semiconductor NCs.[1,2] The integration of MHP NCs into the technological applications, such as solar cells and light-emitting devices, has driven intensive research on characterization and structural control of the properties of excitons.[3−7] Recently, the exciton fine structure of MHP NCs, in particular regarding the access to the dark exciton state whose extremely long lifetime can be beneficial for some applications of photons from exciton, has become a subject of much interest.[8−12]

The optically inactive dark exciton appears as the lowest-energy (ground) exciton state in most semiconductor NCs, therefore, the dark exciton state is populated through the transition from the initially excited bright exciton to dark exciton state. At low temperatures with thermal energy ($kT$) smaller than the bright−dark energy splitting ($\Delta E_{BD}$), a substantial dark exciton population can be obtained giving rise to long-lived photoluminescence (PL) from the radiative relaxation of dark excitons.[13−15] Recently, the reversal of the bright and dark exciton level ordering was reported in cesium lead halide ($CsPbX_3$) NCs, based on the observation of only bright exciton PL in single-particle studies at cryogenic temperatures, indicating the loss of the typical pathway to reach the dark exciton level.[8] On the other hand, a study in $FAPbBr_3$ NCs under magnetic field reported the signature of a dark exciton ∼2.5 meV below the bright exciton level in the single-particle PL spectra.[9] Another study in Mn-doped $CsPbCl_3$ NCs also argued for the dark ground-state exciton from the observation of the weak but longer-lived decay component in the lower-temperature PL.[10] However, because of the dominance of the bright exciton PL even at cryogenic temperatures and the absence of a direct measurement of the dark exciton relaxation, the accessibility to dark exciton as well as its energetic and dynamic characteristics still remains elusive in this new class of semiconductor NCs.

Here, we report the direct observation of intense and long-lived PL with 1−10 $\mu$s lifetime from dark ground exciton state in strongly quantum-confined $CsPbBr_3$ NCs revealing the importance of confinement-enhanced $\Delta E_{BD}$ in gaining facile access to dark exciton. In contrast to MHP NCs studied earlier that were in the weak confinement regime, strongly quantum-confined $CsPbBr_3$ NCs at cryogenic temperatures exhibit the PL primarily from dark exciton. The $\Delta E_{BD}$, determined directly from the PL spectra, is significantly larger than weakly confined $FAPbBr_3$ NCs and strongly confined NCs of many other semiconductors.[9,13,16−18] The larger $\Delta E_{BD}$ in strongly confined $CsPbBr_3$ NCs enables access to the dark exciton at higher temperatures, which is particularly important for the

Received: June 30, 2020
Revised: August 26, 2020
Published: August 26, 2020

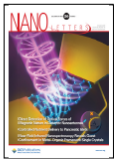







https://dx.doi.org/10.1021/acs.nanolett.0c02714
*Nano Lett.* 2020, 20, 7321−7326

applications of dark exciton. Furthermore, intense dark exciton PL was observed regardless of the dimensionality of the confinement, making all strongly confined 0D (quantum dot), 1D (nanowire,) and 2D (nanoplatelet) NCs viable nanostructures to exploit the dark exciton's longevity. The results from this study demonstrate the potential of strongly quantum-confined MHP NCs as the excellent material platform to utilize dark exciton, combining the benefits of the superb properties of MHP as the source of photons and charges with large confinement-enhanced $\Delta E_{BD}$.

## RESULTS AND DISCUSSION

Figure 1 shows the electron microscopy images and room-temperature optical spectra of weakly confined NCs and

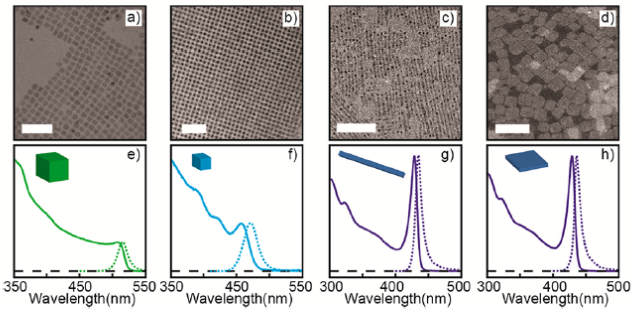


**Figure 1.** Electron microscopy images (a–d) and optical spectra (e–h) of weakly confined NCs ($l$ = 10 nm) and strongly confined QDs ($l$ = 4 nm), NWs ($l \times w$ = 2 × 100 nm), and NPLs ($l \times w \times h$ = 2 × 25 × 25 nm), (left to right). The cartoon depicting the NC morphology and the size are indicated in each panel. Solid and dashed lines in the spectra are for the absorption and photoluminescence, respectively. (a–c) TEM images; (d) STEM image. Dark spots in (c) are formed during TEM imaging likely from the e-beam damage of the NWs. TEM scale bars (a–c) 50 nm (d) 100 nm.

strongly confined quantum dots (QDs), nanowires (NWs), and nanoplatelets (NPLs) of $CsPbBr_3$ used to examine the PL from dark exciton. The size of the NCs in the quantum-confined dimension indicated in Figure 1 for the QDs, NWs, and NPLs is much smaller than twice the exciton Bohr radius of $CsPbBr_3$ ($2a_B$ = 7 nm) imposing strong quantum confinement in varying dimensionality.[1] The weakly confined NCs were prepared following the procedure reported by Protesescu et al.[1] Strongly confined QDs, NWs, and NPLs were synthesized following the methods developed by Dong et al. which can control the size and morphology precisely with high ensemble uniformity, as reflected in the microscopy images and the optical spectra showing the well-defined features of strongly confined excitons.[7,19] For the optical measurements, all of the samples were passivated with dimethyl-dioctadecyl-ammonium bromide (DDAB) via ligand exchange for improved stability and PL quantum yield in polystyrene (PS) matrix used to disperse the NCs for PL measurements. Detailed descriptions of the synthesis and measurement methods are in Sections 2 and 3 of the Supporting Information.

Figure 2 shows the time-resolved PL spectra (a–d), spectrally integrated PL decay dynamics (e–h), and steady-state PL spectra (i–l) following above-bandgap excitation (400 or 405 nm) at 5 K for the four $CsPbBr_3$ NC samples shown in Figure 1. While the PL spectra at 300 K exhibits a single well-defined PL feature which decays on the several ns time scale

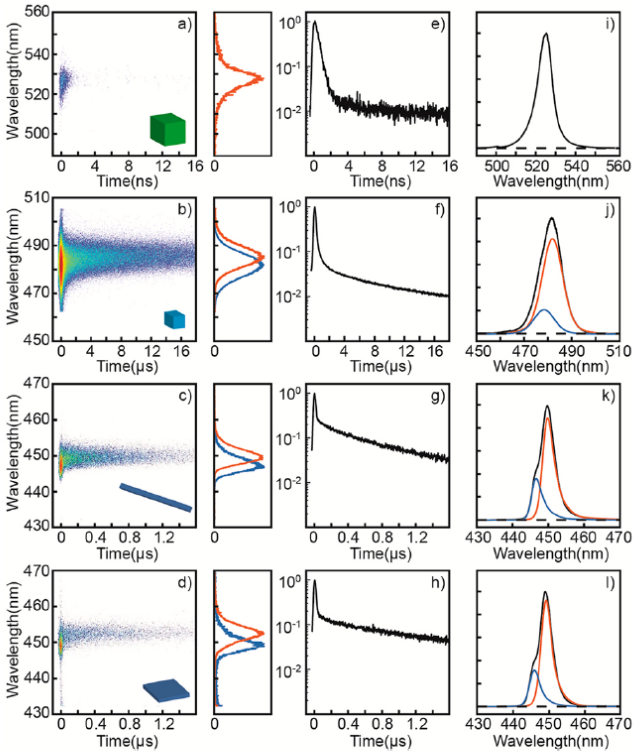


**Figure 2.** Time-resolved PL spectra (a–d), normalized spectrally integrated PL decay dynamics (e–h), and steady-state PL spectra (i–l) of four different $CsPbBr_3$ NCs measured at 5 K. The data are for weakly confined NCs, QDs, NWs, and NPLs from top to bottom. The two spectra shown next to panels b-d are the time-gated PL spectra taken near 0 ps (blue) and 0.5 $\mu$s (red). These two spectra are used to fit the steady-state spectra in (i–l).

for all samples (Figures S1–S4), at 5 K the PL shows very different spectral and dynamic features. In the weakly confined $CsPbBr_3$ NCs, a single PL peak with ~500 ps decay time is observed (Figure 2a,e,i), similar to the results from earlier studies performed at either single-particle or ensemble level.[8,11,20] Because of the intense and fast-decaying PL on the subnanosecond time scale even at 5 K, a recent study by Becker et al. concluded that the dark exciton level is above the bright exciton level which dominates the 5 K PL in $CsPbBr_3$ NCs.[8] On the other hand, a study by Chen et al. concluded that the dark exciton is below the bright exciton level based on the kinetic analysis of the temperature-dependent PL dynamics, although the accuracy of the kinetic model for extracting the relevant parameters needs further scrutiny.[12] In another study by Canneson et al., the same subnanosecond PL observed at 5 K from $CsPbBr_3$ NCs was interpreted as the negative trion PL arising from a charged subpopulation of NCs, with little contribution from the neutral (bright exciton) subpopulation of the NCs.[20] Despite the differences in the interpretation of the PL in different studies, all converged on very weak or lack of dark exciton PL in weakly confined $CsPbBr_3$ NCs.

In contrast, all three strongly confined NCs of varying dimensionalities, that is, QDs, NWs, and NPLs, exhibit two different PL peaks with decay time constants that differ by many orders of magnitude (Figure 2b–d). Time gating the PL spectra near 0 ps and 0.5 $\mu$s readily reveals the two PL peaks separated by 17–22 meV as shown to the right of Figure 2b–d. The fast and slow components of the PL decay kinetics in


https://dx.doi.org/10.1021/acs.nanolett.0c02714
Nano Lett. 2020, 20, 7321–7326

Figure 2f–h with corresponding time constants of $\tau_{fast}$ and $\tau_{slow}$ are associated with the higher-energy and lower-energy PL peaks, respectively. Fitting the steady-state PL spectra (Figure 2j–l) with the two PL peaks indicates that the lower-energy PL constitutes ~70% of the total photons emitted at 5 K in these NCs. We assign the higher-energy and lower-energy PL to the bright and dark excitons respectively, as will be discussed in detail shortly. Since the bright and dark exciton PL are clearly separable in the time-resolved spectra, $\Delta E_{BD}$ is directly determined from the separation between the two PL peaks. Table 1 summarizes $\Delta E_{BD}$, $\tau_{fast}$, and $\tau_{slow}$ of the PL decay

**Table 1. Parameters Extracted from the PL Decay Data at 5 K**[a]

| sample | $\Delta E_{BD}$ (meV) | $\tau_{slow} = \tau_D$ ($\mu$s) | $\tau_{fast}$ (ps) | $\tau_B$ (ps) | $\tau_{BD}$ (ps) | $I_D/I_{tot}$ (%) |
|---|---|---|---|---|---|---|
| QD | 17 | 10 | 387 | 1600 | 510 | 76 |
| NW | 19 | 0.85 | 44 | 160 | 62 | 68 |
| NPL | 22 | 1.2 | 37 | 124 | 54 | 73 |

[a] $\Delta E_{BD}$ and $\tau_D$ were extracted directly from the time-resolved PL spectra and PL decay kinetics. The fraction of dark exciton PL from total PL was obtained by fitting of the steady-state PL spectra. $\tau_B$ and $\tau_{BD}$ were estimated from the analysis of the steady-state PL intensity and $\tau_{fast}$. $\tau_{fast}$ was obtained from short-time window PL data (Figure S8) that provides higher time resolution as detailed in Supporting Information.

kinetics, and the fraction of photons from the dark exciton in the PL at 5 K. Since $\Delta E_{BD}$ is much larger than $kT$ at 5 K, prohibiting thermal excitation from the dark to bright exciton states, $\tau_{slow}$ can reliably be taken as the dark exciton lifetime $\tau_D$. On the other hand, $\tau_{fast}$ reflects the decay of the bright exciton population via radiative and nonradiative relaxation combined with transition between the bright to the dark exciton states. The estimation of the bright exciton lifetime ($\tau_B$) and the time constant for the bright-to-dark transition ($\tau_{BD}$) has been made from the analysis of the relative intensities of the bright and dark exciton PL at 5K with a few assumptions, as described in detail in the Supporting Information.

In Table 1, $\tau_{BD}$ is significantly shorter than $\tau_B$ for all three strongly confined NCs, indicating that dark exciton can be reached effectively from the initially excited bright exciton. This contrasts to the conclusions from the earlier study in organic–inorganic hybrid $FAPbBr_3$ NCs that also have ground dark exciton level with $\Delta E_{BD}$ of 2–3 meV but does not show dark exciton PL in the absence of magnetic field.[9] It was considered that slow bright-to-dark transition is responsible for the difficulty in observing dark exciton PL in the MHP NCs. The present study suggests that the confinement-enhanced $\Delta E_{BD}$ is a more critical factor that determines the accessibility to the dark exciton in $CsPbBr_3$ NCs. The confinement enhancement of $\Delta E_{BD}$ was predicted earlier from a theoretical study and is consistent with the variation of $\Delta E_{BD}$ at 5 K in QDs and NPLs with the degree of quantum confinement observed in this study.[21,22] Figure S6 compares the lower-energy (dark exciton) and higher-energy (bright exciton) PL peaks from the time-resolved PL spectra of three different QDs of varying quantum confinement at 5 K. The data clearly show the increasing $\Delta E_{BD}$ and relative intensity of dark exciton PL with increasing quantum confinement, corroborating the importance of the confinement in obtaining intense dark exciton PL. Figure S7 shows the same trend for NPLs. Therefore, we consider that the stark contrast of the dark exciton PL between the weakly and strongly confined $CsPbBr_3$ NCs at cryogenic temperatures is mainly due to the large $\Delta E_{BD}$ enhanced by confinement.

Temperature-dependent steady-state PL spectra in Figure S5, showing the two well-resolved PL peaks of NWs and NPLs, indicate that the major contribution to the PL is from dark exciton even at ~20 K significantly above liquid helium temperature. This demonstrates potential advantage of large $\Delta E_{BD}$ in utilizing dark exciton PL requiring cryogenic temperatures. It is worth noting that $\Delta E_{BD}$ of $CsPbBr_3$ QDs and NPLs are significantly larger than $\Delta E_{BD}$ of CdSe QDs and NPLs of similar size and thickness, whose exciton fine structure was extensively studied as a prototypical semiconductor NC system. For CdSe QDs, $\Delta E_{BD}$ of 0.8–6 meV was reported for QDs of ~4 nm in diameter and $\Delta E_{BD}$ of 12.5 meV for QDs of 2.4 nm in diameter.[13,17,18] $\Delta E_{BD}$ of 2–4.5 meV was reported for CdSe NPLs of 1.2–1.5 nm in thickness in the literature.[16] Interestingly, $\tau_B$ of NWs (160 ps) and NPLs (124 ps) is nearly an order of magnitude shorter than in QDs. The faster $\tau_B$ in NWs and NPLs compared to QDs is reminiscent of the enhanced exciton recombination rate observed in other 1D and 2D confined semiconductors, reflecting the larger exciton binding energies and enhanced electron–hole correlations.[16,23] Despite the rapid relaxation of bright exciton in NWs and NPLs, even more rapid bright-to-dark transition enables reaching dark exciton as efficiently as in QDs.

The assignment of microseconds-lived lower-energy PL to the dark exciton has been made by ruling out other processes that can produce a PL red-shifted from the bright exciton PL in MHP NCs and performing the magneto fluorescence measurements. Self-trapped exciton, phonon replica, and defect emission have been discussed previously as the origin of red-shifted PL observed in several MHP materials both in bulk and nanocrystalline forms.[24–28] In addition, trion emission or interparticle excimer-like emission has been discussed as the origin of certain PL features red-shifted from the exciton PL in CdSe NPLs and in weakly confined $CsPbBr_3$ NCs.[29–31] These alternative possibilities were ruled out by examining the difference in the spectral characteristics of the PL, such as the line width, lifetime, the magnitude of red shift from the bright exciton, and the dependence of the lifetime on external magnetic field.

Self-trapped exciton has been discussed extensively to explain a broad PL feature red-shifted from the exciton PL observed in some MHP NCs prominent under the subgap excitation condition.[24] PL from the self-trapped exciton typically has a much larger spectral line width and Stokes shift than the exciton PL due to the larger lattice displacement associated with these transitions. In $CsPbBr_3$ NCs, the PL from self-trapped exciton was observed ~100 meV below the exciton PL with a three times broader line width and a lifetime of ~170 ns, very different from the lower-energy PL observed in the strongly confined $CsPbBr_3$ NCs of this study. Furthermore, the disappearance of the self-trapped exciton PL with above-bandgap excitation further rules out self-trapped exciton as the origin for the microseconds-lived lower-energy PL observed in our study. Similarly, phonon overtones are observed in the low-temperature PL spectra for all semiconductors. The first phonon overtone will appear as a PL sideband red-shifted by one optical phonon energy with an intensity proportional to the exciton–phonon coupling. While $\Delta E_{BD}$ in this study is similar in the order of magnitude to the optical phonon energy of bulk $CsPbBr_3$, the large disparity


https://dx.doi.org/10.1021/acs.nanolett.0c02714
Nano Lett. 2020, 20, 7321–7326

between the lifetimes of the two PL peaks by many orders of magnitude immediately dismisses this possibility.

A red-shifted PL feature with similar spectral line width to the exciton PL is often observed in the low-temperature PL spectra of CdSe NPLs. While its origin is still debated, two recent works suggested it may result from the excimer-like emission from stacked NPLs or trion emission.[29,30] Considering that we observed the red-shifted PL universally in all strongly quantum-confined NCs of different dimensionalities, the excimer-like emission observed in CdSe NPLs is not likely to explain our observation in MHP NCs. Trion PL red-shifted from neutral bright exciton PL, reported in weakly confined $CsPbBr_3$ NCs, has subnanoseconds decay time many orders of magnitude shorter than $\mu$s decay time of the lower-energy PL in this study.[31] Furthermore, the independence of the PL lifetime on the magnetic field from these two origins contrasts with the strongly magnetic field-dependent lifetime of the slow-decay component in the PL shown in Figure 3, further ruling out these two options.

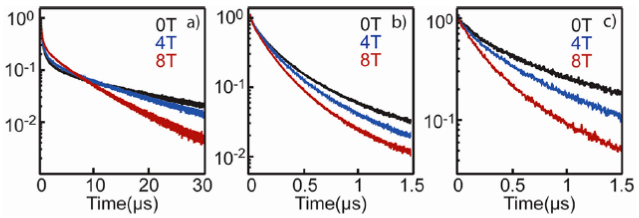


**Figure 3.** Magnetic field-dependent PL decay dynamics of $CsPbBr_3$ QDs (a), NWs (b), and NPLs (c) at liquid helium temperature. Only the slow-decay component of the PL decaying on a microseconds-time-scale is plotted for NWs and NPLs since 150 ns excitation pulse interferes with correct interpretation of the fast component decaying in <50 ps. For QDs with ~400 ps fast-decay component, the entire PL decay kinetics are shown.

Figure 3 shows the dependence of the slow-decay component of the PL from $CsPbBr_3$ QDs, NWs, and NPLs under 0T, 4T, and 8T magnetic field at liquid helium temperature. For all three of the strongly confined NCs, the lifetime of the slow-decay component assigned to dark exciton PL shortens with increasing magnetic field. The shorting of the lifetime is consistent with the expected behavior of the dark exciton, which results from the mixing of the bright and dark state by the magnetic field. The similar trend of magnetic field dependence of the dark exciton lifetime was observed in recent studies on single $FAPbBr_3$ NCs and Mn-doped $CsPbCl_3$ NC ensembles.[9,10] For self-trapped exciton, defect emission, trion emission, and excimer-like emission, the dependence of the PL lifetime on the magnetic field is not expected, as has been experimentally confirmed in several studies.[29,30] In addition to the discussion above, the shortening of the PL lifetime under the magnetic field supports decisively the assignment of the lower-energy PL with 1−10 $\mu$s lifetime to the dark exciton.

In order to gain further insights into the competitive dynamics of the exciton relaxation and bright-to-dark transition and to check if parameters in Table 1 determined from the spectra at 5 K are valid beyond 5 K, the temperature-dependent $\tau_{fast}$ and $\tau_{slow}$ were analyzed with a kinetic model as shown in Figure 4a. Under this simple kinetic model, $\tau_{fast}$ and $\tau_{slow}$ at each temperature are determined by the competition of the relaxation of bright and dark excitons separated by $\Delta E_{BD}$ and the temperature-dependent reversible transition between bright and dark states as explained in detail in Supporting Information. Often, $\Delta E_{BD}$ and time constants ($\tau_B$, $\tau_D$, and $\tau_{BD}$) are extracted as the best fitting parameters of the temperature-dependent $\tau_{fast}$ and $\tau_{slow}$ to the kinetic model, when these cannot not be directly determined from the time-resolved spectra unlike in this study.[10,18,20,32] If the kinetic model accounts for all the dynamic processes in the NCs studied here ideally, the model should reproduce $\tau_{fast}$ and $\tau_{slow}$ from the $\Delta E_{BD}$ and time constants in Table 1.

Figure 4b−d compares $\tau_{fast}$ and $\tau_{slow}$ of QDs, NWs, and NPLs with the calculated values using the model in the temperature range of 5−100 K. The details of calculation are in Supporting Information. For QDs, the temperature dependence of $\tau_{fast}$ and $\tau_{slow}$ are well reproduced with the kinetic model using $\Delta E_{BD}$, $\tau_B$, $\tau_D$, and $\tau_{BD}$ in Table 1 as nonadjustable parameters up to 100 K. This indicates that the kinetic model is reasonably satisfactory for describing the exciton dynamics in QDs and that $\Delta E_{BD}$ and the time constants determined from 5 K spectra are valid in the higher temperature ranges. The same analysis for NWs and NPLs reproduces $\tau_{slow}$ quite well, while $\tau_{fast}$ shows more discrepancy between the measured and calculated values from the model. The rapid change of the experimentally measured $\tau_{fast}$ in 5−20 K suggests the possible involvement of an additional nonradiative decay channel for the exciton in NWs and NPLs that is not accounted for in the kinetic model employed here. Since $\tau_{fast}$ is more sensitive to $\tau_B$ and $\tau_{BD}$ than to $\tau_D$, the temperature dependence of $\tau_B$ is the most likely culprit. The larger discrepancy of the measured and calculated $\tau_{fast}$ in NWs and NPLs compared to the QDs is also consistent with the more complicated and larger temperature dependence of the relative PL QY in NWs and NPLs (Figure S9).

## ■ CONCLUSION

Our results present clear evidence for the readily accessible dark ground exciton state in strongly quantum-confined $CsPbBr_3$ NCs. In contrast to weakly confined NCs, strongly confined QDs, NWs, and NPLs of $CsPbBr_3$ exhibit intense and long-lived dark exciton PL < ~20 K due to the large confinement-enhanced splitting between bright and dark

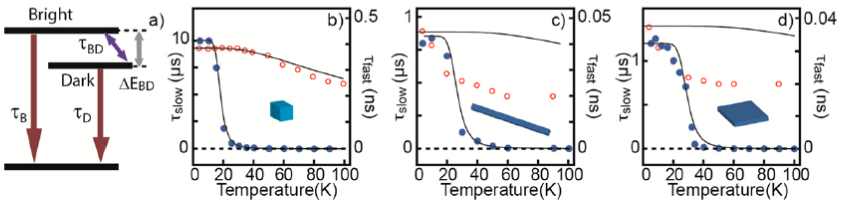


**Figure 4.** Kinetic model (a) used to analyze the temperature dependence of $\tau_{fast}$ (○) and $\tau_{slow}$ (●) from QDs (b), NWs (c), and NPLs (d). Curves are the values calculated using the kinetic model and nonadjustable parameters in Table 1.



https://dx.doi.org/10.1021/acs.nanolett.0c02714
Nano Lett. 2020, 20, 7321−7326

states. This result establishes the exciting possibility to take advantage of the superior photonic properties of strongly confined MHPs in the applications utilizing long-lived dark states.

## ■ ASSOCIATED CONTENT

### Supporting Information

The Supporting Information is available free of charge at https://pubs.acs.org/doi/10.1021/acs.nanolett.0c02714.

Experimental details including the list of chemicals, sample synthesis, time-resolved and steady-state PL measurement, magnetofluorescence measurement, additional temperature-dependent PL dyanmics data, and details of the kinetic analysis (PDF)

## ■ AUTHOR INFORMATION


### Corresponding Authors

**Dong Hee Son** − *Department of Chemistry, Texas A&M University, College Station, Texas 777843, United States; Center for NanoMedicine, Institute for Basic Science (IBS), Seoul 03722, Republic of Korea;* orcid.org/0000-0001-9002-5188; Email: dhson@chem.tamu.edu

**Jinwoo Cheon** − *Center for NanoMedicine, Institute for Basic Science (IBS), Seoul 03722, Republic of Korea; Department of Chemistry and Graduate Program of Nano Biomedical Engineering (BME), Advanced Science Institute, Yonsei University, Seoul 03722, Republic of Korea;* orcid.org/0000-0001-8948-5929; Email: jcheon@yonsei.ac.kr

### Authors

**Daniel Rossi** − *Center for NanoMedicine, Institute for Basic Science (IBS), Seoul 03722, Republic of Korea*

**Xiaohan Liu** − *Department of Physics, Texas A&M University, College Station, Texas 777843, United States*

**Yangjin Lee** − *Center for NanoMedicine, Institute for Basic Science (IBS), Seoul 03722, Republic of Korea; Department of Physics, Yonsei University, Seoul 03722, Republic of Korea;* orcid.org/0000-0001-7336-1198

**Mohit Khurana** − *Department of Physics, Texas A&M University, College Station, Texas 777843, United States*

**Joseph Puthenpurayil** − *Department of Chemistry, Texas A&M University, College Station, Texas 777843, United States*

**Kwanpyo Kim** − *Center for NanoMedicine, Institute for Basic Science (IBS), Seoul 03722, Republic of Korea; Department of Physics, Yonsei University, Seoul 03722, Republic of Korea;* orcid.org/0000-0001-8497-2330

**Alexey V. Akimov** − *Department of Physics, Texas A&M University, College Station, Texas 777843, United States; Russian Quantum Center, Moscow 143025, Russia; PN Lebedev Institute RAS, Moscow 119991, Russia;* orcid.org/0000-0002-4167-5085

Complete contact information is available at: https://pubs.acs.org/10.1021/acs.nanolett.0c02714


### Author Contributions

D.H.S. conceived the idea for the study. D.R. synthesized the materials and performed the low-temperature streak measurements. X.L. and M.K. performed the low-temperature magnetic field measurements under the supervision of A.A. Y.L. performed the TEM measurement under the supervision of K.K. and J.C. D.R. and D.H.S. wrote the manuscript. All authors discussed the results and commented on the manuscript. D.H.S. and J.C. supervised the project.

### Notes

The authors declare no competing financial interest.

## ■ ACKNOWLEDGMENTS

D.H.S. and A.A. acknowledge the National Science Foundation (CHE-1836538) and X-grants from Texas A&M University for financial support. J.C. acknowledges Institute for Basic Science (IBS-R026-D1) for financial support.

## ■ REFERENCES


(1) Protesescu, L.; Yakunin, S.; Bodnarchuk, M. I.; Krieg, F.; Caputo, R.; Hendon, C. H.; Yang, R. X.; Walsh, A.; Kovalenko, M. V. Nanocrystals of cesium lead halide perovskites ($CsPbX_3$, X = Cl, Br, and I): novel optoelectronic materials showing bright emission with wide color gamut. *Nano Lett.* **2015**, *15* (6), 3692−3696.

(2) Stranks, S. D.; Eperon, G. E.; Grancini, G.; Menelaou, C.; Alcocer, M. J. P.; Leijtens, T.; Herz, L. M.; Petrozza, A.; Snaith, H. J. Electron-hole diffusion lengths exceeding 1 micrometer in an organometal trihalide perovskite absorber. *Science* **2013**, *342* (6156), 341−344.

(3) Yakunin, S.; Protesescu, L.; Krieg, F.; Bodnarchuk, M. I.; Nedelcu, G.; Humer, M.; De Luca, G.; Fiebig, M.; Heiss, W.; Kovalenko, M. V. Low-threshold amplified spontaneous emission and lasing from colloidal nanocrystals of caesium lead halide perovskites. *Nat. Commun.* **2015**, *6* (1), 8056.

(4) Wu, K.; Liang, G.; Shang, Q.; Ren, Y.; Kong, D.; Lian, T. Ultrafast interfacial electron and hole transfer from $CsPbBr_3$ perovskite quantum dots. *J. Am. Chem. Soc.* **2015**, *137* (40), 12792−12795.

(5) Utzat, H.; Sun, W.; Kaplan, A. E. K.; Krieg, F.; Ginterseder, M.; Spokoyny, B.; Klein, N. D.; Shulenberger, K. E.; Perkinson, C. F.; Kovalenko, M. V.; Bawendi, M. G. Coherent single-photon emission from colloidal lead halide perovskite quantum dots. *Science* **2019**, *363* (6431), 1068−1072.

(6) Nedelcu, G.; Protesescu, L.; Yakunin, S.; Bodnarchuk, M. I.; Grotevent, M. J.; Kovalenko, M. V. Fast anion-exchange in highly luminescent nanocrystals of cesium lead halide perovskites ($CsPbX_3$, X = Cl, Br, I). *Nano Lett.* **2015**, *15* (8), 5635−5640.

(7) Dong, Y.; Qiao, T.; Kim, D.; Parobek, D.; Rossi, D.; Son, D. H. Precise control of quantum confinement in cesium lead halide perovskite quantum dots via thermodynamic equilibrium. *Nano Lett.* **2018**, *18* (6), 3716−3722.

(8) Becker, M. A.; Vaxenburg, R.; Nedelcu, G.; Sercel, P. C.; Shabaev, A.; Mehl, M. J.; Michopoulos, J. G.; Lambrakos, S. G.; Bernstein, N.; Lyons, J. L.; Stöferle, T.; Mahrt, R. F.; Kovalenko, M. V.; Norris, D. J.; Rainò, G.; Efros, A. L. Bright triplet excitons in caesium lead halide perovskites. *Nature* **2018**, *553* (7687), 189−193.

(9) Tamarat, P.; Bodnarchuk, M. I.; Trebbia, J.-B.; Erni, R.; Kovalenko, M. V.; Even, J.; Lounis, B. The ground exciton state of formamidinium lead bromide perovskite nanocrystals is a singlet dark state. *Nat. Mater.* **2019**, *18* (7), 717−724.

(10) Xu, K.; Vliem, J. F.; Meijerink, A. Long-lived dark exciton emission in Mn-Doped $CsPbCl_3$ perovskite nanocrystals. *J. Phys. Chem. C* **2019**, *123* (1), 979−984.

(11) Rainò, G.; Nedelcu, G.; Protesescu, L.; Bodnarchuk, M. I.; Kovalenko, M. V.; Mahrt, R. F.; Stöferle, T. Single cesium lead halide perovskite nanocrystals at low temperature: fast single-photon emission, reduced blinking, and exciton fine structure. *ACS Nano* **2016**, *10* (2), 2485−2490.

(12) Chen, L.; Li, B.; Zhang, C.; Huang, X.; Wang, X.; Xiao, M. Composition-dependent energy splitting between bright and dark excitons in lead halide perovskite nanocrystals. *Nano Lett.* **2018**, *18* (3), 2074−2080.

(13) Nirmal, M.; Norris, D. J.; Kuno, M.; Bawendi, M. G.; Efros, A. L.; Rosen, M. Observation of the "dark exciton" in CdSe quantum dots. *Phys. Rev. Lett.* **1995**, *75* (20), 3728−3731.
(14) Schaller, R. D.; Crooker, S. A.; Bussian, D. A.; Pietryga, J. M.; Joo, J.; Klimov, V. I. Revealing the exciton fine structure of PbSe nanocrystal quantum dots using optical spectroscopy in high magnetic fields. *Phys. Rev. Lett.* **2010**, *105* (6), 067403.
(15) Li, Z.; Wang, T.; Jin, C.; Lu, Z.; Lian, Z.; Meng, Y.; Blei, M.; Gao, S.; Taniguchi, T.; Watanabe, K.; Ren, T.; Tongay, S.; Yang, L.; Smirnov, D.; Cao, T.; Shi, S.-F. Emerging photoluminescence from the dark-exciton phonon replica in monolayer $WSe_2$. *Nat. Commun.* **2019**, *10* (1), 2469.
(16) Biadala, L.; Liu, F.; Tessier, M. D.; Yakovlev, D. R.; Dubertret, B.; Bayer, M. Recombination dynamics of band edge excitons in quasi-two-dimensional CdSe nanoplatelets. *Nano Lett.* **2014**, *14* (3), 1134−1139.
(17) Crooker, S. A.; Barrick, T.; Hollingsworth, J. A.; Klimov, V. I. Multiple temperature regimes of radiative decay in CdSe nanocrystal quantum dots: Intrinsic limits to the dark-exciton lifetime. *Appl. Phys. Lett.* **2003**, *82* (17), 2793−2795.
(18) de Mello Donegá, C.; Bode, M.; Meijerink, A. Size- and temperature-dependence of exciton lifetimes in CdSe quantum dots. *Phys. Rev. B: Condens. Matter Mater. Phys.* **2006**, *74* (8), 085320.
(19) Dong, Y.; Qiao, T.; Kim, D.; Rossi, D.; Ahn, S. J.; Son, D. H. Controlling anisotropy of quantum-confined $CsPbBr_3$ nanocrystals by combined ese of equilibrium and kinetic anisotropy. *Chem. Mater.* **2019**, *31* (15), 5655−5662.
(20) Canneson, D.; Shornikova, E. V.; Yakovlev, D. R.; Rogge, T.; Mitioglu, A. A.; Ballottin, M. V.; Christianen, P. C. M.; Lhuillier, E.; Bayer, M.; Biadala, L. Negatively charged and dark excitons in $CsPbBr_3$ perovskite nanocrystals revealed by high magnetic fields. *Nano Lett.* **2017**, *17* (10), 6177−6183.
(21) Sercel, P. C.; Lyons, J. L.; Wickramaratne, D.; Vaxenburg, R.; Bernstein, N.; Efros, A. L. Exciton fine structure in perovskite nanocrystals. *Nano Lett.* **2019**, *19* (6), 4068−4077.
(22) Ramade, J.; Andriambariarijaona, L. M.; Steinmetz, V.; Goubet, N.; Legrand, L.; Barisien, T.; Bernardot, F.; Testelin, C.; Lhuillier, E.; Bramati, A.; Chamarro, M. Fine structure of excitons and electron-hole exchange energy in polymorphic $CsPbBr_3$ single nanocrystals. *Nanoscale* **2018**, *10* (14), 6393−6401.
(23) Tessier, M. D.; Javaux, C.; Maksimovic, I.; Loriette, V.; Dubertret, B. Spectroscopy of single CdSe nanoplatelets. *ACS Nano* **2012**, *6* (8), 6751−6758.
(24) Ma, X.; Pan, F.; Li, H.; Shen, P.; Ma, C.; Zhang, L.; Niu, H.; Zhu, Y.; Xu, S.; Ye, H. Mechanism of single-photon upconversion photoluminescence in all-inorganic perovskite nanocrystals: the role of self-trapped excitons. *J. Phys. Chem. Lett.* **2019**, *10* (20), 5989−5996.
(25) Lao, X.; Yang, Z.; Su, Z.; Wang, Z.; Ye, H.; Wang, M.; Yao, X.; Xu, S. Luminescence and thermal behaviors of free and trapped excitons in cesium lead halide perovskite nanosheets. *Nanoscale* **2018**, *10* (21), 9949−9956.
(26) Iaru, C. M.; Geuchies, J. J.; Koenraad, P. M.; Vanmaekelbergh, D.; Silov, A. Y. Strong carrier-phonon coupling in lead halide perovskite nanocrystals. *ACS Nano* **2017**, *11* (11), 11024−11030.
(27) Wu, X.; Trinh, M. T.; Niesner, D.; Zhu, H.; Norman, Z.; Owen, J. S.; Yaffe, O.; Kudisch, B. J.; Zhu, X. Y. Trap states in lead iodide perovskites. *J. Am. Chem. Soc.* **2015**, *137* (5), 2089−2096.
(28) Fu, M.; Tamarat, P.; Trebbia, J.-B.; Bodnarchuk, M. I.; Kovalenko, M. V.; Even, J.; Lounis, B. Unraveling exciton-phonon coupling in individual $FAPbI_3$ nanocrystals emitting near-infrared single photons. *Nat. Commun.* **2018**, *9* (1), 3318.
(29) Diroll, B. T.; Cho, W.; Coropceanu, I.; Harvey, S. M.; Brumberg, A.; Holtgrewe, N.; Crooker, S. A.; Wasielewski, M. R.; Prakapenka, V. B.; Talapin, D. V.; Schaller, R. D. Semiconductor nanoplatelet excimers. *Nano Lett.* **2018**, *18* (11), 6948−6953.
(30) Shornikova, E. V.; Yakovlev, D. R.; Biadala, L.; Crooker, S. A.; Belykh, V. V.; Kochiev, M. V.; Kuntzmann, A.; Nasilowski, M.; Dubertret, B.; Bayer, M. Negatively charged excitons in CdSe nanoplatelets. *Nano Lett.* **2020**, *20* (2), 1370−1377.
(31) Fu, M.; Tamarat, P.; Huang, H.; Even, J.; Rogach, A. L.; Lounis, B. Neutral and Charged Exciton Fine Structure in Single Lead Halide Perovskite Nanocrystals Revealed by Magneto-optical Spectroscopy. *Nano Lett.* **2017**, *17* (5), 2895−2901.
(32) Labeau, O.; Tamarat, P.; Lounis, B. Temperature dependence of the luminescence lifetime of single CdSeZnS quantum dots. *Phys. Rev. Lett.* **2003**, *90* (25), 257404−257408.


https://dx.doi.org/10.1021/acs.nanolett.0c02714
*Nano Lett.* 2020, 20, 7321−7326